J. Fluid Mech. (1978), *vol.* 85, *part* 1, *pp.* 187–192
Printed in Great Britain

Visual observations of the flow past a sphere at Reynolds numbers between 10^4 and 10^6

By S. TANEDA

Research Institute for Applied Mechanics, Kyushu University, Fukuoka 812, Japan

(Received 3 May 1977)

The wake configuration of a sphere has been determined by means of the surface oil-flow method, the smoke method and the tuft-grid method in a wind tunnel at Reynolds numbers ranging from 10^4 to 10^6. It was found that the wake performs a progressive wave motion at Reynolds numbers between 10^4 and $3{\cdot}8 \times 10^5$, and that it forms a pair of streamwise line vortices at Reynolds numbers between $3{\cdot}8 \times 10^5$ and 10^6.

1. Introduction

The literature on sphere flow has been reviewed by Torobin & Gauvin (1959) and Achenbach (1974).

The variation of the wake structure with Reynolds number is as follows. When the Reynolds number is lower than about 20, the flow is laminar everywhere and separation does not occur (Taneda 1956). At Reynolds numbers between about 20 and 400 a stationary vortex ring is formed at the rear of the sphere (Möller 1938; Taneda 1956; Achenbach 1974). When a Reynolds number of about 400 is reached, the vortex ring begins to oscillate, and the wake forms horseshoe-shaped vortex loops at Reynolds numbers between about 400 and 10^3 (Möller 1938; Magarvey & MacLatchy 1965; Achenbach 1974). At Reynolds numbers above about 10^3 the vortex loops diffuse very rapidly, and little seems to be known about the wake configuration (Möller 1938; Achenbach 1974; Pao & Kao 1977). For Reynolds numbers higher than about 10^4 no visual observations have so far been reported.

On the other hand, hot-wire measurements have indicated that there exist strong periodic fluctuations in the wake right up to the critical Reynolds number 3×10^5 at which a sharp decrease in the drag coefficient occurs, and that the periodic fluctuations cease when the critical Reynolds number is exceeded (Cometta 1957; Achenbach 1974). It has also been found that at Reynolds numbers between 6×10^3 and 3×10^5 the vortex separation point rotates around the sphere (Achenbach 1974). However, the information obtained from the hot-wire measurements seems to be not yet sufficient to describe the wake structure. It should be noted here that helical and double helical wake configurations are contradictory to Thomson's circulation theorem.

The object of the present experiment was to determine the wake structure of a sphere at Reynolds numbers above 10^4 by means of flow-visualization methods.

2. Apparatus and experimental method

The experiments were carried out in a wind tunnel of single-return-flow type with a closed working section of cross-section 400 × 200 cm. The wind velocity can be varied from 0·1 to 60 m/s. The turbulence level is 0·12 %. A hollow sphere 33 cm in diameter was used as the test sphere. It was made of polyvinyl chloride and was finished black. The diameter tolerance was about 0·01 cm, and no measurable deformation was detected at the maximum wind velocity (50 m/s). Although there was a fine trace of seam from a mould, the height of the trace was less than 0·001 cm. In order to avoid interference by the support system, the sphere was supported from the rear by a small steel rod 1·2 cm in diameter and 63 cm in length. The rod was fixed horizontally on the centre-line of the test section by fine suspension wires 0·5 mm in diameter.

The flow was visualized by the surface oil-flow method, the smoke method and the tuft-grid method. The oil-flow method was used for visualization of the skin-friction distribution over the test sphere. The oil was a mixture of paraffin oil and titanium dioxide. The oil film forms streaks under the combined action of gravity and of the skin friction resulting from the air flow. The pattern of the streaks therefore provides information about the distribution of skin friction over the surface of the sphere. The smoke method was used to observe the behaviour of the wake. Titanium tetrachloride is liquid at normal temperature and reacts with moisture present in the airstream to form visible fumes. If a few drops of the liquid are placed on the rear of the sphere, dense white smoke is generated in the near-wake recirculating region and the wake flow is made visible. To determine the three-dimensional structure of the wake, the flow was photographed simultaneously from two directions at right angles. The tuft-grid method was used to observe the wake in the cross-wind plane at various distances downstream of the sphere. Two tuft grids, 100 × 100 cm with a 5 cm mesh and 60 × 60 cm with a 3 cm mesh, were used in the present experiment.

3. Results

Flow visualization by the surface oil-flow method

Figure 1 (plate 1) shows side views of oil-flow patterns on a sphere at Reynolds numbers $R = 2{\cdot}3 \times 10^5$, $3{\cdot}5 \times 10^5$, $4{\cdot}7 \times 10^5$ and $9{\cdot}2 \times 10^5$. The oil pattern in figure 1 (*a*) shows that at $R = 2{\cdot}3 \times 10^5$ the boundary layer separates at $\phi = 80°$, where ϕ is measured from the front stagnation point. The position of separation remains almost unaltered over the range $10^4 < R < 3{\cdot}5 \times 10^5$. When the Reynolds number is raised to about $3{\cdot}5 \times 10^5$ (figure 1*b*), the oil-flow pattern changes suddenly and three conspicuous lines make their appearance at about $\phi = 100°$, 117° and 135°. They are the laminar separation line, the reattachment line and the turbulent separation line respectively. It will be seen that weak reverse flow exists from 100 to 117°, and that the local skin friction from 117 to 135° is much stronger than that from 0 to 100°. The boundary layer is laminar as far as $\phi = 100°$, but turbulent from 117 to 135°. A separation bubble containing a vortex ring extends from $\phi = 100°$ to $\phi = 117°$. It should be noted here that the above-mentioned positions of the three separation and reattachment lines are average values. As will be seen from figure 1 (*b*), the position of laminar separation varies from 92 to 110° round the sphere, that of reattachment from 107 to 127° and that of turbulent separation from 123 to 147°. The size of the separation bubble decreases as R is

increased (figures 1*c*, *d*). Achenbach (1972) measured the local skin-friction distribution with a skin-friction probe in the Reynolds number range 5×10^4 to 6×10^6. There is fair agreement between his results and ours. Figure 2 (plate 2) shows a surface oil-flow pattern as seen from downstream at $R = 4{\cdot}7 \times 10^5$. An Ω-shaped line ending in a pair of spiral points can be seen. The Ω-shaped line is thought to be the line of attachment of streamlines. It should be noted that the flow is not axisymmetric.

Flow visualization by the smoke method

Figures 3–5 (plates 3–5) show examples of the smoke photographs obtained. The time of photographic exposure for the smoke pictures was $\frac{1}{60}$ s. The smoke was generated at the junction between the sphere and the supporting rod.

Figures 3(*a*) and 4(*a*) show the sphere wake at $R = 2{\cdot}3 \times 10^4$. It will be seen that the near-wake recirculating region is large and the wake performs a progressive wave motion. The wavelength is about $4{\cdot}5d$, where d is the sphere diameter. In order to determine the three-dimensional structure of the waving wake, the smoke was photographed simultaneously from above and from the side. Figure 5 shows top and side views at $R = 2{\cdot}3 \times 10^4$. It is evident that the wake performs a progressive wave motion in a plane which contains an axis through the centre of the sphere in the direction of the undisturbed flow. The plane in which the wake oscillates rotates slowly and irregularly about that axis. The orientation of the plane with respect to the sphere seems to be purely a matter of chance. The wavelength and the shape of the wake remain almost unchanged in the range $10^4 < R < 3{\cdot}8 \times 10^5$.

The Strouhal number can be calculated from the wavelength and the wave velocity. The wave velocity estimated from the photographs taken by double exposure is about $0{\cdot}9U$ in the range $10^4 < R < 3 \times 10^5$, where U is the velocity of the undisturbed flow. Then we find that the Strouhal number is about 0·20 in the range $10^4 < R < 3 \times 10^5$. The Strouhal number found here is in good agreement with that measured with hot wires by Cometta (1957) and Achenbach (1974) at Reynolds numbers between 6×10^3 and 3×10^5. This indicates that the strong periodicity detected by Cometta and Achenbach can be ascribed to the progressive wave motion of the wake. However, the relationship between the observations by Achenbach (1974) of a periodic rotation of the separation point and the present observations of irregular rotation of the plane containing the wake is still a matter of speculation.

When R reaches about $3{\cdot}8 \times 10^5$, the near-wake recirculating region shrinks suddenly and the progressive wave motion ceases. This is also the critical Reynolds number at which the sharp decrease in the drag coefficient occurs. It is evident that the sharp reduction in drag coefficient is due to the shrinkage of the near-wake recirculating region. The critical Reynolds number at which the near-wake recirculating region shrinks is a little higher than that obtained by the oil-flow method. This is due to the fact that the oil-flow method influences the boundary layer slightly. Figures 3(*b*) and 4(*b*) show the sphere wake at $R = 5{\cdot}8 \times 10^5$. The wake flow is fully turbulent. However, in figures 3(*b*) and 4(*b*) there is no appearance of small-scale turbulence, because the smoke travels about 40 cm during the photographic exposure ($\frac{1}{60}$ s). It should be noted that the wake flow is offset from the streamwise axis through the centre of the sphere. This shape of wake flow remains unaltered in the range $3{\cdot}8 \times 10^5 < R < 10^6$. This indicates that a sphere is subjected to a side force in the range $3{\cdot}8 \times 10^5 < R < 10^6$.

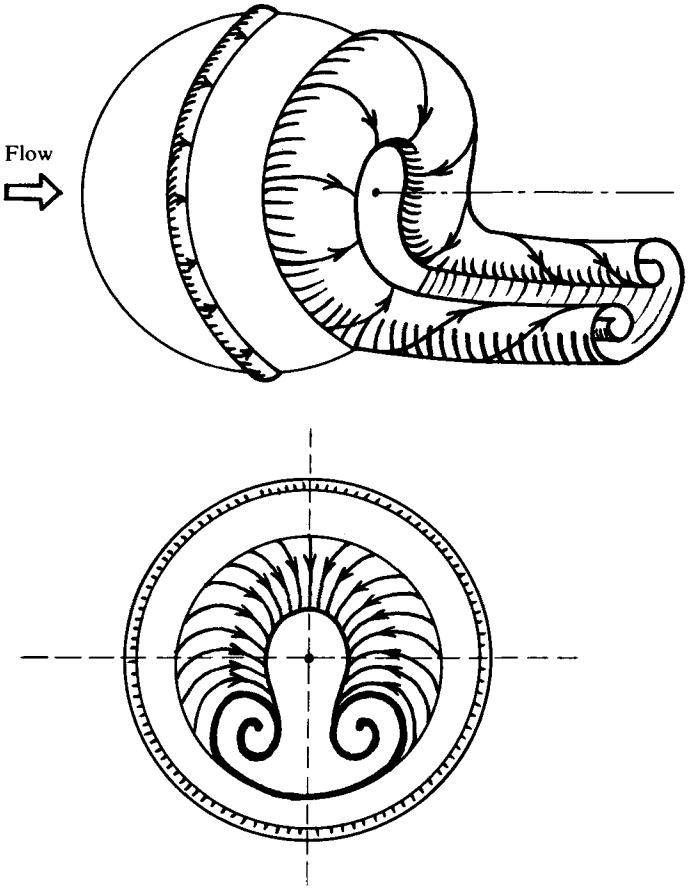

FIGURE 8. Schematic representation of vortex structure in the range $3{\cdot}8 \times 10^5 < R < 10^6$. (The lines marked with arrows show the streamlines on the vortex sheet.)

It is well known that above the critical Reynolds number a sphere experiences a side force (Scoggins 1967).

Flow visualization by the tuft-grid method

Figure 6 (plate 6) shows the tuft patterns in the cross-wind plane 33 cm downstream of the sphere. The regions where the tufts are confused indicate the position and size of the wake cross-section. When R is lower than $3{\cdot}8 \times 10^5$, the diameter of the wake is a little larger than the diameter of the sphere (figure 6*a*). On the other hand, when R is higher than $3{\cdot}8 \times 10^5$, the wake diameter is much smaller than the sphere diameter (figure 6*b*). Figure 7 (plate 7) shows the structure of the wake 6·6 cm downstream of the sphere at $R = 4{\cdot}7 \times 10^5$ in more detail. Comparison of the tuft patterns with the corresponding oil-flow patterns and smoke patterns shows that the wake consists of two oppositely rotating vortices which trail from near the spiral points in the oil-flow pattern on the surface of the sphere. What is very interesting is that the vortex pair is offset from the streamwise axis through the centre of the sphere. The orientation of the wake is influenced by means of small perturbations of the shape of the sphere, or small

obstructions in the wake. For example, when a small stud 0·3 cm in diameter and 1 cm in height was attached to the sphere surface at $\phi = 90°$, the spiral points formed just behind the stud at $R = 4{\cdot}7 \times 10^5$.

Figure 8 shows a sketch of the vortex sheets separating from a sphere in the range $3{\cdot}8 \times 10^5 < R < 10^6$. The vortex sheet shed from the sphere rolls up to form a pair of streamwise vortices. As can be seen in figure 4 (*b*), the vortex pair is shifted outwards by the mutual interaction of the vortices. Although the wake flow is steady in the range $3{\cdot}8 \times 10^5 < R < 5 \times 10^5$, it begins to rotate irregularly about the streamwise axis through the centre of the sphere at $R = 5 \times 10^5$. Clockwise rotations and counterclockwise rotations occur randomly, usually through less than 180° in the range

$$5 \times 10^5 < R < 10^6.$$

There are no definite periodicities, but the mean value of the frequency with which the sense of rotation changes is about 0·5 Hz at $U = 40$ m/s ($R = 9{\cdot}2 \times 10^5$).

4. Conclusions

To determine the wake structure of a sphere at high Reynolds numbers, visualization experiments were carried out in a 400 × 200 cm wind tunnel. The experimental range of Reynolds numbers was from 10^4 to 10^6. For flow visualization the oil-flow method, the smoke method and the tuft-grid method were used.

At Reynolds numbers ranging from 10^4 to $3{\cdot}8 \times 10^5$ the sphere wake performs a progressive wave motion in a plane containing the streamwise axis through the centre of the sphere. The plane rotates slowly and irregularly about that axis. The wavelength equals about 4·5 times the sphere diameter.

At Reynolds numbers ranging from $3{\cdot}8 \times 10^5$ to 10^6, the sphere wake forms a pair of streamwise line vortices at a short distance from the streamwise axis. The vortex pair rotates slowly and randomly about that axis.

What is interesting is that at all Reynolds numbers ranging from about 400 to 10^6 the sphere wake is not axisymmetric. This indicates that a sphere placed in a uniform flow is subjected to a side force at Reynolds numbers between 400 and 10^6. The direction of the side force is completely random.

The author would like to express his thanks to Mr H. Amamoto, Mr K. Ishi-i and Mrs K. Ishimura for their much appreciated assistance. This work was supported by the Grant-in-Aid for Fundamental Scientific Research from the Ministry of Education.

REFERENCES

ACHENBACH, E. 1972 Experiments on the flow past spheres at very high Reynolds numbers. *J. Fluid Mech.* **54**, 565–575.

ACHENBACH, E. 1974 Vortex shedding from spheres. *J. Fluid Mech.* **62**, 209–221.

COMETTA, C. 1957 An investigation of the unsteady flow pattern in the wake of cylinders and spheres using a hot wire probe. *Div. Engng, Brown Univ. Tech. Rep.* WT-21.

MAGARVEY, R. H. & MACLATCHY, C. S. 1965 Vortices in sphere wakes. *Can. J. Phys.* **43**, 1649–1656.

MÖLLER, W. 1938 Experimentelle Untersuchung zur Hydrodynamik der Kugel. *Phys. Z.* **39**, 57–80.

PAO, H. P. & KAO, T. W. 1977 Vortex structure in the wake of a sphere. *Phys. Fluids* **20**, 187–191.

SCOGGINS, J. R. 1967 Sphere behavior and the measurement of wind profiles. *N.A.S.A. Tech. Note* D-3994.

TANEDA, S. 1956 Experimental investigation of the wake behind a sphere at low Reynolds numbers. *J. Phys. Soc. Japan* **11**, 1104–1108.

TOROBIN, L. B. & GAUVIN, W. H. 1959 Fundamental aspect of solids–gas flow. Part II. The sphere wake in steady laminar fluids. *Can. J. Chem. Engng* **37**, 167–176.

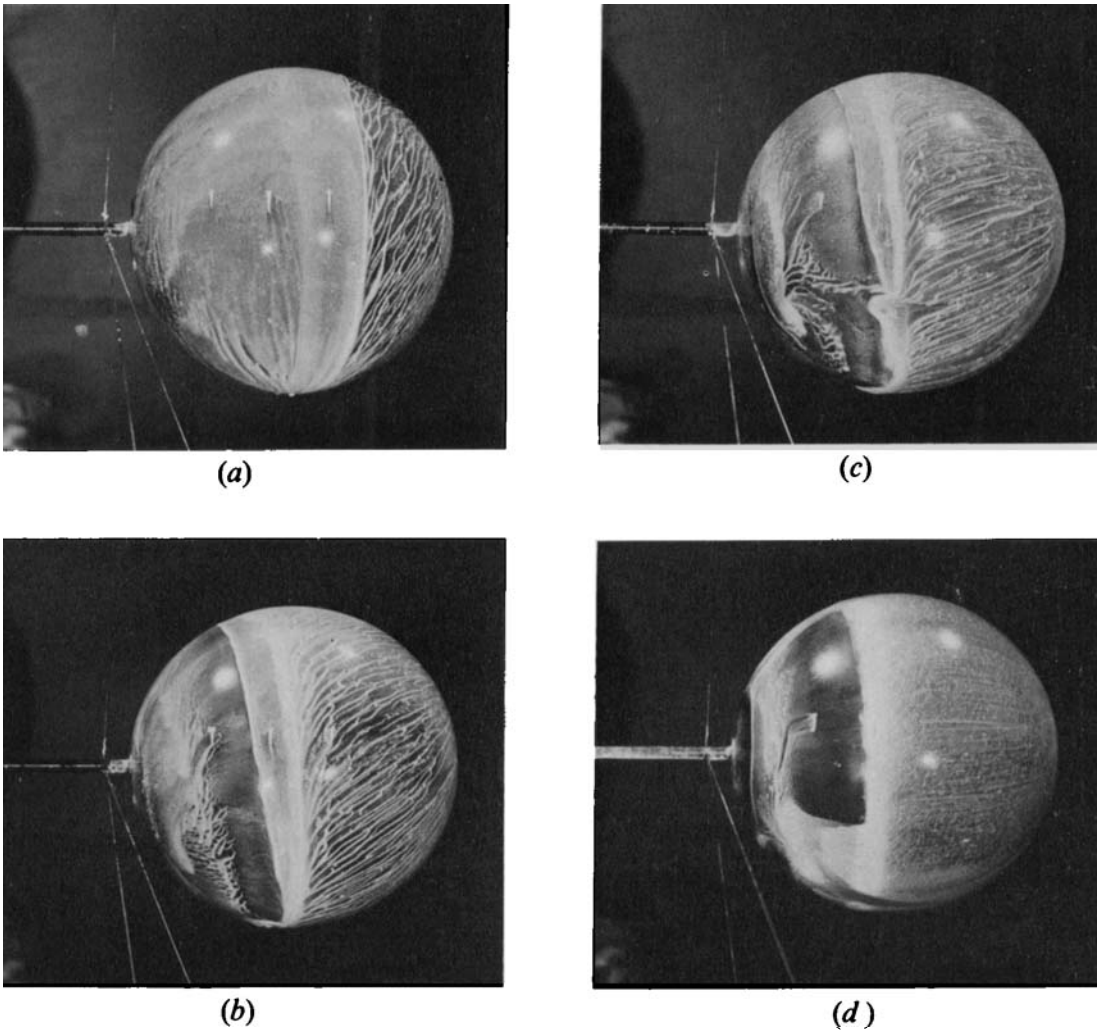

FIGURE 1. Oil-flow patterns. Air is flowing from right to left. (*a*) $R = 2{\cdot}3 \times 10^5$. (*b*) $R = 3{\cdot}5 \times 10^5$. (*c*) $R = 4{\cdot}7 \times 10^5$. (*d*) $R = 9{\cdot}2 \times 10^5$.

(*Facing p.* 192)

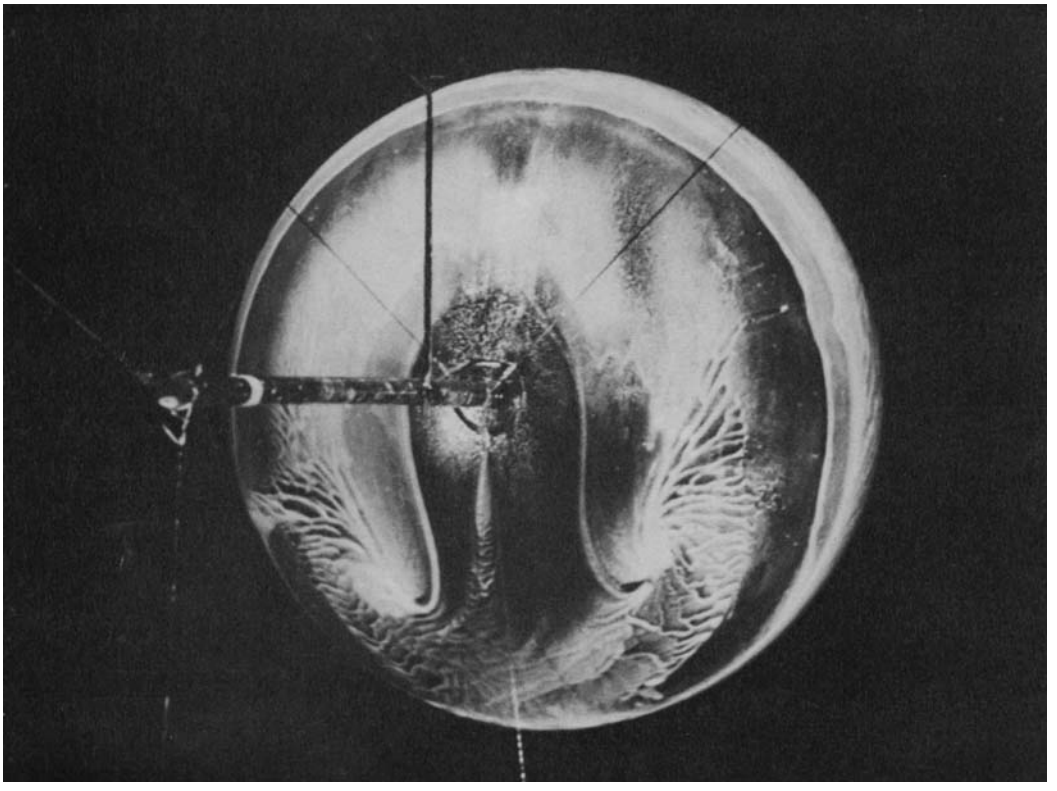

FIGURE 2. Oil-flow pattern on the rear surface. $R = 4{\cdot}7 \times 10^5$.

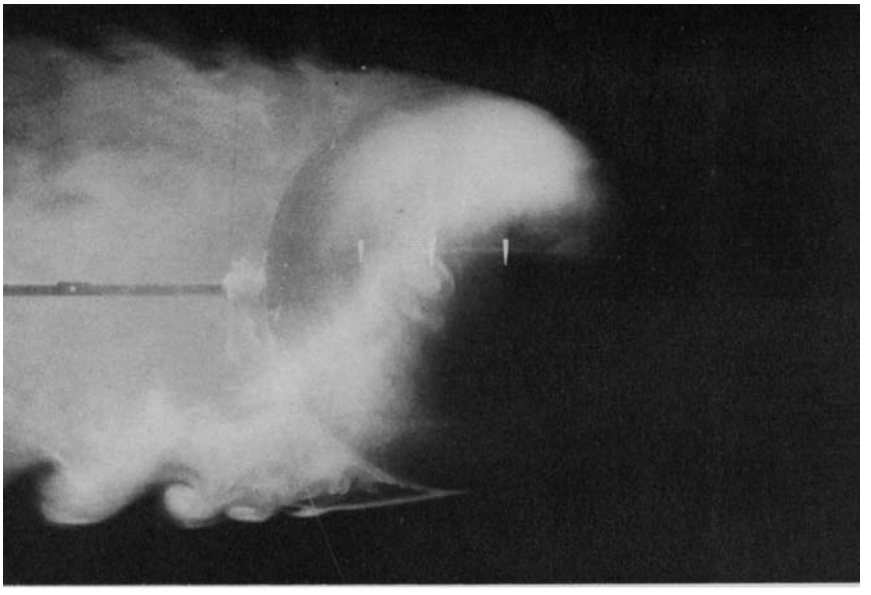

(*a*)

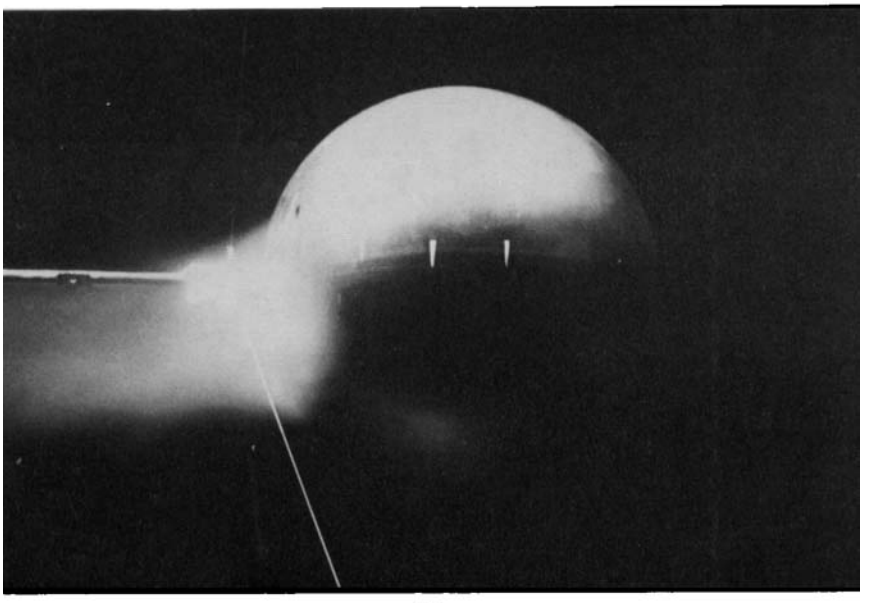

(*b*)

FIGURE 3. Smoke photographs. (*a*) $R = 2{\cdot}3 \times 10^4$. (*b*) $R = 5{\cdot}8 \times 10^5$.

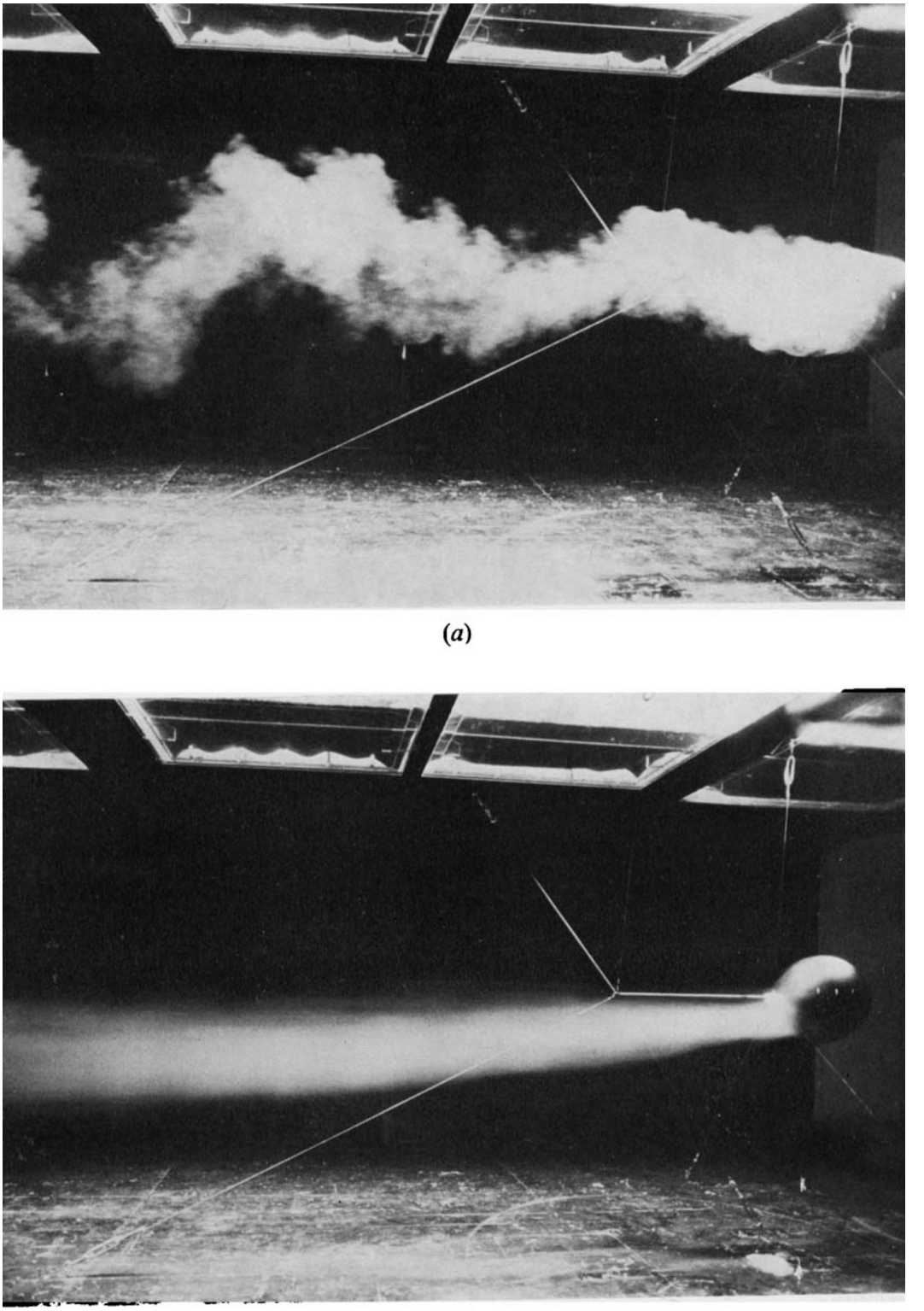

(*a*)

(*b*)

FIGURE 4. Photographs of smoke in the wake. (*a*) $R = 2{\cdot}3 \times 10^4$. (*b*) $R = 5{\cdot}8 \times 10^5$.

(*a*)

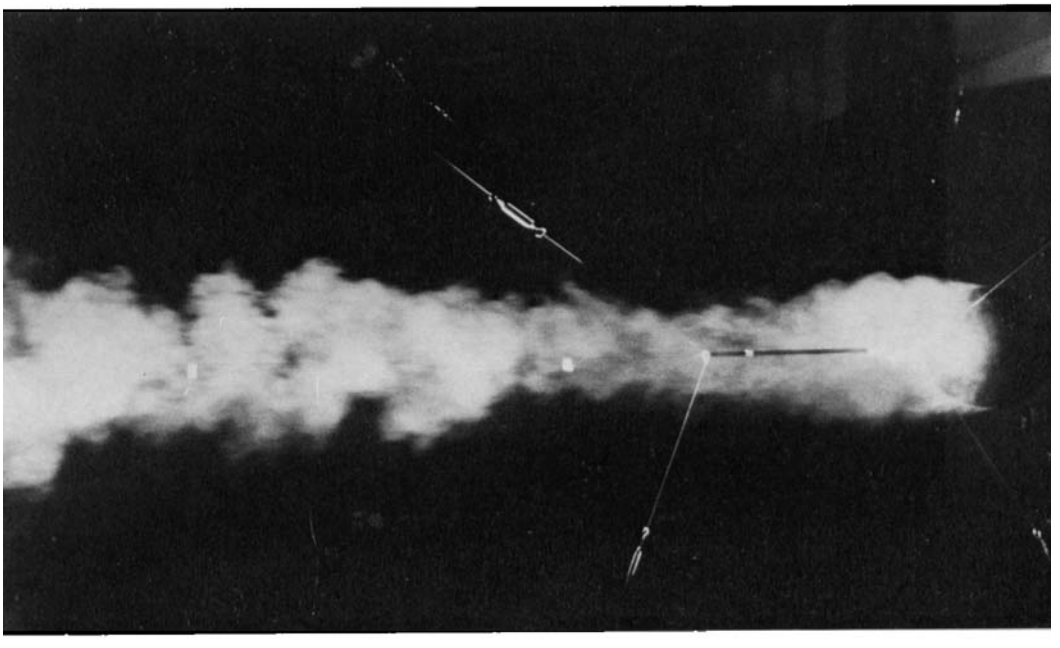

(*b*)

FIGURE 5. Simultaneous smoke photographs from above and from the side. $R = 2{\cdot}3 \times 10^4$. (*a*) Top view. (*b*) Side view.

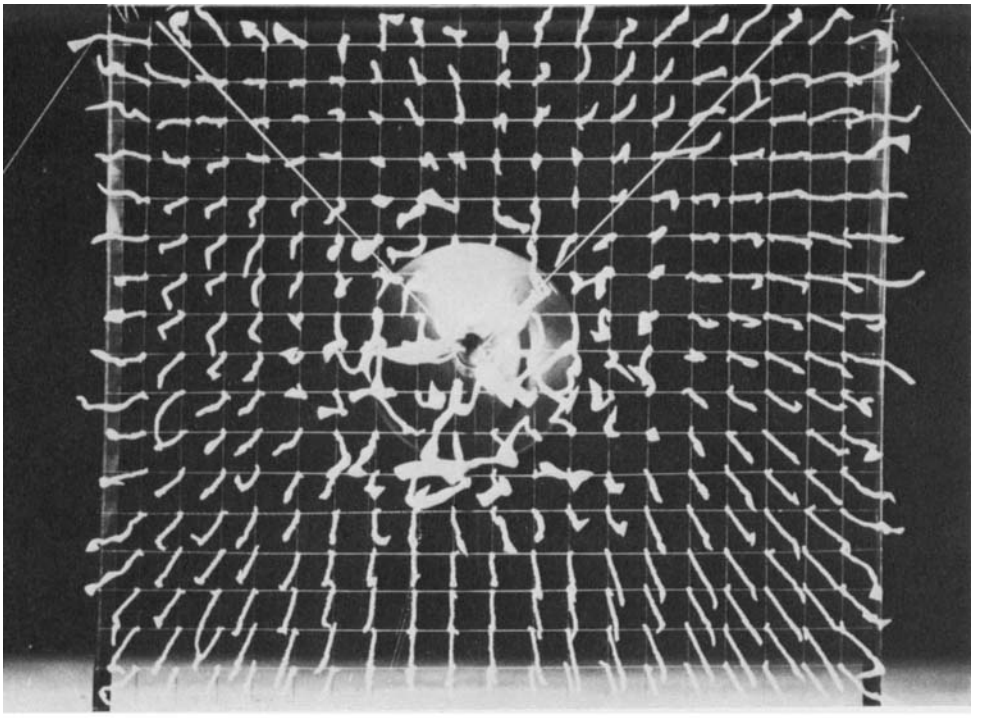

(*a*)

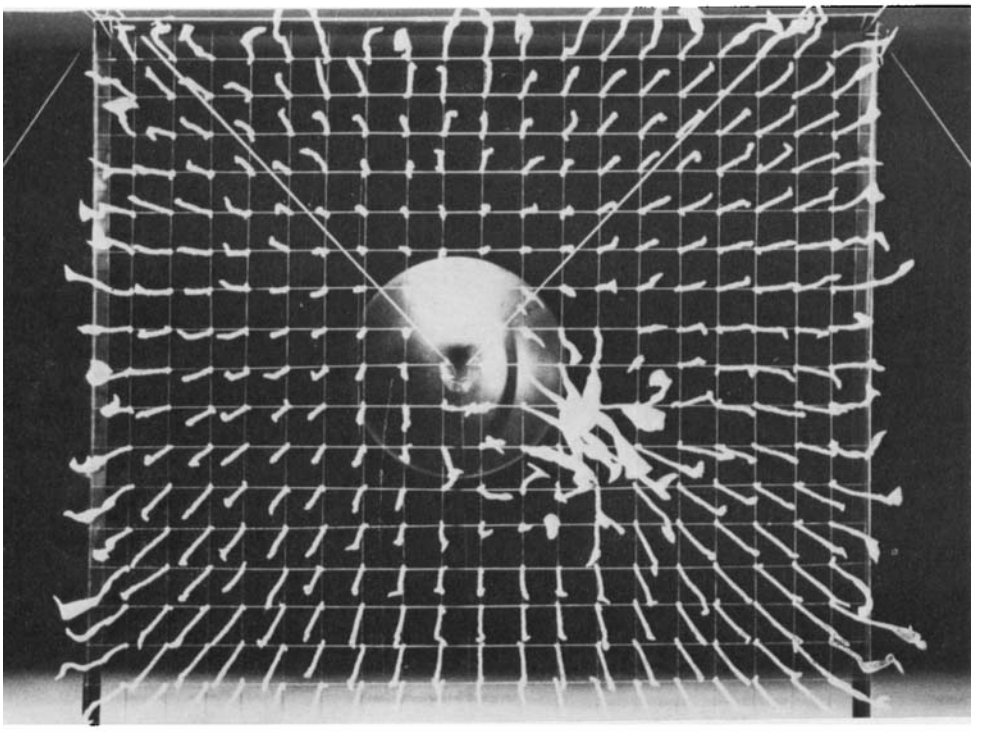

(*b*)

FIGURE 6. Tuft patterns 33 cm downstream of the sphere. (Tuft grid: 100 × 100 cm with 5 cm mesh.) (*a*) $R = 2{\cdot}3 \times 10^5$. (*b*) $R = 4{\cdot}7 \times 10^5$.

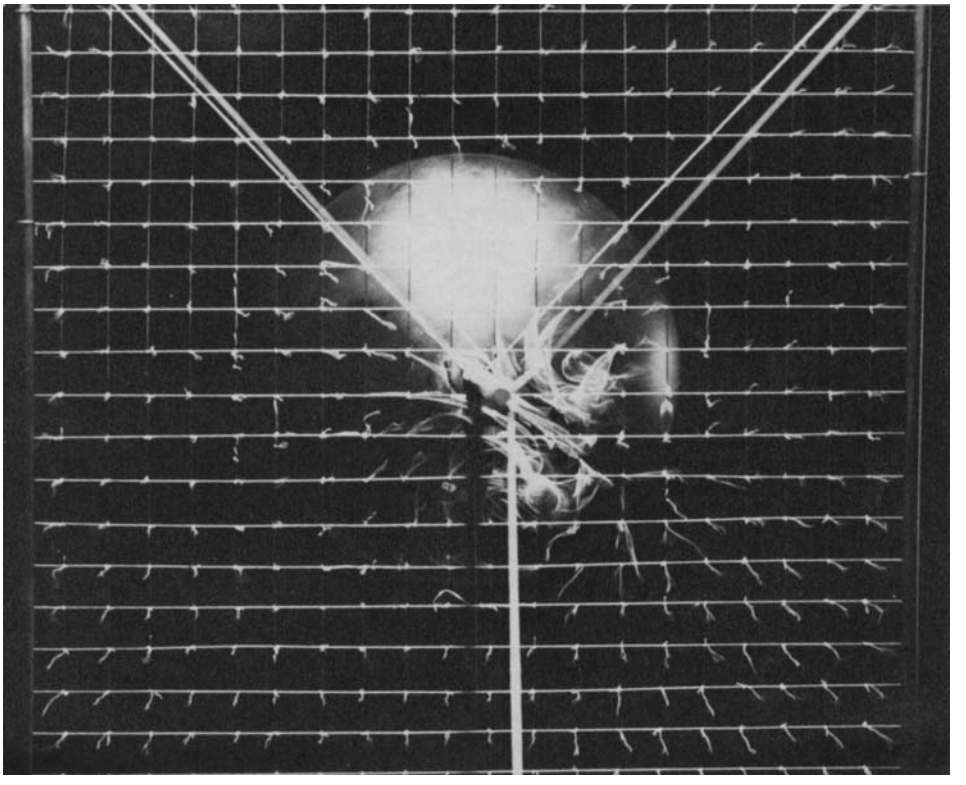

FIGURE 7. Tuft pattern 6·6 cm downstream of the sphere. $R = 4{\cdot}7 \times 10^5$.
(Tuft grid: 60×60 cm with 3 cm mesh.)